X-625-72-171

PREPRINT

NASA TM X- 65913

AN ATLAS OF LOW LATITUDE 6300A (OI) NIGHT AIRGLOW FROM OGO-4 OBSERVATIONS

EDITH I. REED
WALTER B. FOWLER
JACQUES E. BLAMONT

MAY 1972

GSFC
GODDARD SPACE FLIGHT CENTER
GREENBELT, MARYLAND

AN ATLAS OF LOW LATITUDE 6300A [OI] NIGHT AIRGLOW FROM OGO-4 OBSERVATIONS

by

Edith I. Reed
Laboratory for Planetary Atmospheres

Walter B. Fowler
Laboratory for Optical Astronomy
NASA/Goddard Space Flight Center
Greenbelt, Maryland 20771

and

Jacques E. Blamont
Service d'Aeronomie
Centre National de la Recherche Scientifique
Boite Postale No. 3
91 - Verrieres le Buisson
France

NOTE

This document is similar to, but not identical with a manuscript prepared for submission to the Journal of Geophysical Research. In this document, black and white maps are substituted for the Color Plates of the journal manuscript. Furthermore Color Plate 1 is for November 18-20 instead of November 22-25, Color Plate 4 is for December 25-28 instead of December 29-30, and the curves in Figure 7 are for the corresponding dates. The general content of the maps is similar except that less moonlight was present in the original data for the dates used in the JGR color plates. The advantage of ready reproduction of black and white maps is felt to outweigh the change of dates.

ABSTRACT

The atomic oxygen emission line at 6300A as measured in the nadir direction by a photometer on the polar orbiting satellite OGO-4 has been plotted between 40^{o}N and 40^{o}S latitude on a series of maps for the moon-free periods between August 30, 1967 and January 10, 1968. Readily apparent are the longitudinal and local time variations which occur during the northern fall-winter season. The northern tropical arc is more widespread; the southern arc is not present at all longitudes. The arcs in early evening are strong and distinct, separated by very low emission rates at the magnetic equator. The arcs lie generally along magnetic parallels, move toward the magnetic equator as the night progresses, and, in the early morning hours, decrease in emission rate and degenerate into patches. Regions of enhanced emissions, corresponding to a sunlit atmosphere in the conjugate area, are found both in the evening and in the morning. The paper describes the conditions under which the observations were made as well as presenting four airglow maps selected to show the local time variations.

INTRODUCTION

The observations of the 6300A emission line of atomic oxygen $O(^1D \rightarrow ^3P)$ on a world-wide basis from satellite-borne photometers offers a unique method of probing the atmosphere at altitudes near 300 km. At night at low latitudes the $O(^1D)$ is primarily the result of a two step process:

$$O^+ + O_2 \rightarrow O_2^+ + O \qquad \text{followed by}$$

$$O_2^+ + e \rightarrow O + O(^1D)$$

The $O(^1D)$, which has a radiative lifetime of 110 seconds, will at altitudes below about 250 km begin to lose its energy to the neutral molecules by collisional deexcitation. Hence the 6300A emission is a reflection of the vertical distribution of both the neutral and ionized components of the atmosphere.

The use of observations of 6300A has been limited by the few low latitude airglow observatories in operation in any given year and by the fact that many of the movements of interest are on a scale too large to be effectively studied from a single station. Satellite observations can be used for such features and give a geographic coverage on a scale hitherto unattainable.

It is the purpose of this paper to present a selection of OGO-4 (Orbiting Geophysical Observatory) observations of the 6300A airglow, and describe instrumental and operational limitations which govern their content. The various low and mid-latitude phenomena evident in the OGO-4 data are discussed and related to the detailed and long term data available at specific locations.

The emission rate of 6300A as a function of latitude and longitude at various local times is presented in a series of maps. The observations were made by the earth-looking airglow photometer on OGO-4 from August 1967 through January 1968. Besides giving an overall view of low latitude airglow and its large scale phenomena, the maps also serve as an index to available OGO-4 airglow data. Detailed data, including that for other wavelengths, are available in limited amounts from the authors. All data will eventually be placed in the National Space Science Data Center (Greenbelt, Maryland 20771).

MAIN BODY PHOTOMETER

The Main Body Photometer on OGO-4 was designed to measure the integrated vertical emission and had the following characteristics:

1. Emission was measured in 6 different wavelength regions below the spacecraft and in one (6300A) above the spacecraft. The expected sources of light in each region are given in Table 1.

2. Spectral bandpass for visual wavelengths was a nominal 50 A and for the uv (2630 A) region was about 250 A.

3. Minimum detectable signal (for 5577 A) was less than 5 Rayleighs.

4. Photometer output was measured with an accuracy ranging from 4 to 10% between the minimum detectable signal

TABLE 1

WAVELENGTH Region, A	SOURCES OF LIGHT	
2630 (2500-2750)	$O_2(A^3\Sigma_u^+)$ Herzberg	airglow
	$N_2(A^3\Sigma_u^+)$ Vegard-Kaplan	aurora
3914	$N_2^+(B^2\Sigma_u^+)$ First Negative	aurora
	unidentified band (Broadfoot & Kendall, 1968)	airglow
	Hg	mercury vapor street lamps
5577	$O(^1S)$	airglow and aurora
	OH(7-1) Meinel	airglow
5893	$Na(^2P)$	airglow sodium vapor street lamps
	OH(8-2) Meinel	airglow
	$N_2(B^3\pi_g)$ first positive	aurora
6225	OH(9-3) Meinel	airglow
6300	$O(^1D)$	airglow and aurora
	OH(9-3) Meinel	airglow

In addition, an airglow continuum is present in the 5577, 5893, 6225, and 6300A regions. A second continuum source for these same regions and the 3914A is that due to starlight, zodiacal light, and moonlight reflected from the earth and its atmosphere. The continuum from incandescent street lamps appears in the 5577, 5893, 6225, and 6300 A regions. When the spacecraft is sunlit, scattered sunlight can appear in all regions. Measurements above the spacecraft were made in the 6300A region, in which the (O^1D) emission, starlight, zodiacal light, and moonlight could be detected.

and the upper limit of about 200 kilorayleighs. Absolute accuracy of radiance was about 15%.

5. The field of view had a half angle slightly less than 5 degrees.

6. A complete set of measurements was made in 8 seconds, corresponding to a movement by the spacecraft along the orbit of about 1/2 degree of latitude.

7. Appropriate protection was provided to avoid photocathode and dynode fatigue and damage from direct or earth reflected solar illumination.

8. Although the instrument was designed primarily for use with the spacecraft in the earth's shadow, baffling was sufficient for some low brightness measurements when the spacecraft was sunlit; skyward measurements could be made when the sun was more than 60^{o} from zenith. A more detailed description of the characteristics of the instrument is given in (Reed, Fowler & Blamont, 1972). A brief report of the results from a similar instrument in OGO-2 is given in Reed and Blamont, 1967. An analysis of OGO-4 data from a meteorological viewpoint is given in Warnecke, et al., 1969; observations of the moonlit earth are used to determine earth albedo by Fowler et al., 1971. A description of the moving mechanisms (shutters, stepper motors, etc.) is given in Bauernschub, 1965.

CALIBRATION

Prior to flight the spectral responsivity was measured over the expected range of radiances and operating temperatures (0 to 40^{o} C).

The spectral characteristics of each wavelength interval, determined primarily by the interference filter, are given for room temperature in Table 2. The temperature effects were due partly to the wavelength shift in filter characteristics and partly to the change in responsivity of the photomultiplier and its electronics. The absolute responsivity and its temperature coefficients for a continuum source and for line sources at the nominal wavelengths are given in Table 3.

The responsivity over the entire range of the photometer was checked and found to be linear with variations of less than 4% for radiances corresponding to anode currents of up to 4×10^{-7} amperes. Above this, the nearly logarithmic curve was experimentally determined.

Careful measurements were made of the wings of the spectral response curve of the photometer by noting the response in each of the mirror positions relative to a high radiance of near monochromatic light corresponding to each one of the wavelength regions. The relative responses were arbitrarily termed crosstalk coefficients and are given in Table 4.

TABLE 2. Spectral characteristics of each channel.

Channel	Wavelength (Å) at stated relative responsivity							
	0.01	0.1	0.5	1.0	0.5	0.1	0.01	Effective bandpass
1	2250	2436	2554	2652	2778	2920	3118	258
2	6240.5	6267	6284.5	6303	6319.5	6336.2	6364	40
3	6238.5	6262.3	6279.0	6298.5	6319.5	6334.5	6360.5	44
4	6139.5	6179.7	6201.7	6229.5	6257.0	6279.7	6320.7	59
5	5818.8	5846.0	5864.0	5885.0	5905.5	5921.7	5951.7	45
6	5487	5526.8	5549.0	5574.0	5600.2	5625.5	5670	57
7	3847.5	3881.0	3900.2	3924.5	3946.2	3965.0	3997	49

TABLE 3

Mirror Position	Nominal Wavelength	Conversion factor continuum	Conversion factor line	Temperature coeff. continuum	Temperature coeff. line	Background coefficient	Field of view Half-angle	Field of view area
1	2630 A	61.75		9.6×10^{-3}			$4^{\circ}51'$	0.0220
2	6300 A	474	195.4	1.6×10^{-2}	1.04×10^{-2}		$3^{\circ}23'$	0.0109
3	6300 A	226	99	3.6×10^{-3}	1.04×10^{-2}	0.7	$4^{\circ}27'$	0.0190
4	6225 A	162.6		3.6×10^{-3}			$4^{\circ}42'$	0.0211
5	5892 A	160.8	75.8	3.6×10^{-3}	6.0×10^{-3}	1.2	$4^{\circ}54'$	0.0229
6	5577 A	89.3	51.3	3.6×10^{-3}	8.8×10^{-3}	1.5	$4^{\circ}41'$	0.0210
7	3914 A	85.4	49.3	3.6×10^{-3}	1.4×10^{-2}		$4^{\circ}52'$	0.0227

TABLE 3. Response and field of view of the airglow photometer. The conversion factors are in Rayleighs per 100 A per volt for continuum and in Rayleighs per volt for line emissions. The temperature coefficient is the change of the responsivity per degree centigrade divided by the responsivity at 25° C. The background coefficient multiplies the continuum observation in volts in mirror position 4 for the corresponding background measurement that would be estimated for another mirror position. The area of the field of view is in steradians.

TABLE 4

Relative response to light in the passband of the stated mirror position

	1	2	3	4	5	6	7
1	1.0	2.5×10^{-4}	0	2.5×10^{-5}	1.5×10^{-5}	$5. \times 10^{-6}$	0
2	0	1.0	0	2.7×10^{-5}	$5. \times 10^{-6}$	1.3×10^{-6}	0
3	0	1.6×10^{-4}	1.0	0	$5. \times 10^{-4}$	6.6×10^{-4}	$3. \times 10^{-4}$
4	0	1.0×10^{-5}	2.5×10^{-2}	1.0	$8. \ 10^{-3}$	8.6×10^{-4}	4.2×10^{-4}
5	0		$9. \times 10^{-4}$	2.8×10^{-3}	1.0	5.7×10^{-4}	1.9×10^{-3}
6	0	1.6×10^{-6}	1.6×10^{-5}	2.7×10^{-4}	2.3×10^{-2}	1.0	4.4×10^{-4}
7	0	1.6×10^{-6}	0	0	$3. \times 10^{-6}$	3.3×10^{-5}	1.0

Table 4. Crosstalk coefficients: the relative response of the photometer to near-monochromatic light corresponding to each of the stated mirror positions. The light scattered into mirror position 0 due to a continuum source was taken to be 5×10^{-5} times the response in channel 7.

The absolute responsivity was measured in May 1966 with NBS calibrated quartz-iodine lamps and a large area white diffuser. Further checks included photomultipliers and thermopiles calibrated by the Eppley Laboratory. The resultant responsivity is represented by 1.0 on the ordinate in Figure 1. Final ground calibration, after a year of environmental testing, was based on three stable C^{14} excited phosphors of approximately the same spectral radiance as the airglow. These phosphors were periodically calibrated both against our standard lamps and by M. Gadsden and H.V. Blacker at ESSA in Boulder, Colorado. Accuracy of laboratory and phosphor calibration is estimated at ±5%. By May 1967, the responsivity had dropped equally for all filter channels to 85% of its May 1966 value.

After launch three techniques were used to measure responsivity. Ground observations made at 6300 A and 5577 A on clear nights in early October from the Haleakala Airglow Observatory in Hawaii were compared with OGO-4 data taken when the satellite was within 75^{o} of zenith (Smith 1970). See Figure 2. At 6300 A, after making appropriate computations concerning the geometry and background emissions, it was noted that the responsivity over the range of 40 to 350 Rayleighs had dropped to 64% of the 1966 value. The airglow emission on one of the three passes used was sufficiently featureless so that with several assumptions concerning altitudes and relative emission rates, it was possible to

make a comparison of the satellite and ground observations of the E-region 5577 emissions; the resulting responsivity relative to the May 1966 calibration was 65%.

A second inflight technique was the observation at 6300 A of overhead bright stars or planets. Irradiance was obtained for stars by interpolation with respect to class and wavelength in a table of monochromatic magnitudes (Code, 1960) in general conformance with the methods given by Roach (1956) and Ramsey (1962). In the case of planets, use was made of visual stellar magnitude from the American Ephemeris and Nautical Almanac, curves of planetary spectral reflectivity (Harris 1961), and Arveson's values for the solar spectra (1969). The results of observing various stars and planets as well as the comparison with ground observations are plotted in Figure 1. It is believed that the absolute responsivity of the photometer as given by Table 3 with Figure 1 is known to an accuracy of $\pm$ 7%.

A third inflight technique involved observation of the highest radiance over clouds and the lowest radiance over ocean under conditions near full moon (phase between $\pm 30^{o}$). Computed lunar spectral irradiance at the sub-satellite point was used to compute bidirectional reflectance which was then compared to atmospheric models for an approximate absolute calibration (Fowler, et al 1971).

Because change of responsivity was slow, the relative drop in responsivity, as plotted in Figure 1, could also be observed in moonlit bidirectional reflectance data and was found to be the same on all channels viewing moonlight below the spacecraft.

The various prelaunch calibrations indicated that the change of responsivity as a function of time was the same at all wavelengths. The comparison with data from Haleakala taken through much narrower interference filters tends to indicate that the responsivity of the photometer changed equally for both 5577 A and 6300 A. The change in response to an internal incandescent lamp was similar for all channels, further indicating that the responsivity of the various channels with respect to each other probably remained constant in flight.

For the analysis of OGO-4 flight data through March 31, 1968, the relative responsivity, R, was computed by the formula

$$R = \exp\ (-1.477 \times 10^{-3}\ N + 2.217 \times 10^{-2})$$

where N is the number of days and is equal to 1 on January 1, 1967.

DATA REDUCTION AND ANALYSIS

The signal at the photomultiplier cathode was expressed in terms of the voltage that would have appeared across the anode resistor if the gain of the photomultiplier had remained constant and at the laboratory reference conditions. To do this, the most sensitive on-scale word of the three electrometer outputs was converted to voltage and adjusted for the gain of the photomultiplier appropriate to the value of the high voltage monitor. If the signal was above the linear ranges of the system, the value of the high voltage monitor was converted using the experimentally determined curve.

To eliminate the transients occurring each time the mirror stepped from one position to the next, the data in the first 300 milliseconds of each second were deleted. To delete pulses due to energetic particles and lightning, the remaining samples were arranged in ascending order and the average taken of the lowest $(n/3)+1$ samples (n is the number of samples in the last 700 milliseconds). If there were only two samples, the lower of the two was used.

The value of the dark current to be subtracted was found by interpolating between the measurements of dark current made at 8 second intervals. For the 6300A data presented in this paper background emissions due to continuum, OH bands, and reflected starlight and zodiacal light were removed by subtracting 0.7 times the voltage observed in the

6225 A channel. The factor of 0.7 was arrived at by considering the nightglow spectrum given by Broadfoot and Kendall (1968), the spectrum of the stars and zodiacal light as equivalent to a G-2 star, a nominal earth albedo of 0.4, and the responsivity of the photometer in the 6225 A and 6300 A channels. It is a compromise value which does not take into account the fact that the spectra of the background as observed from a satellite changes appreciably with earth albedo. Neither does the present method of data analysis take into account the apparent increase in line emission rate due to high earth albedo (e.g. clouds, snow, or ice), which could give results which are high by as much as a factor of two for an earth albedo equal to 1.0. However, these emissions would not appreciably alter the general pattern of the tropical red arcs, which have about a factor of 10 more emission than the mid-latitude red airglow. After correcting for dark current and for background emissions, the resulting value for photocathode current was multiplied by a conversion factor derived from Table 3 and Figure 1 to arrive at the emission in terms of rayleighs.

The photometer observations derived from playback data for the non-moonlit periods have been plotted on microfilm such that each frame contains the data for one channel for one day over a 30^{o} range of latitude. The data from a number of frames of microfilm have been reassembled to make the 6300 A airglow maps which appear later in this paper.

The systematic and random errors introduced by neglect of temperature changes (over a range of about 5° C), neglect of crosstalk contributions, and noise is judged to be less than $\pm$ 15%.

OPERATIONS

The availability of data from the photometer depended on a number of factors, some dependent on orbit parameters such as the presence of moonlight and sunlight, and others dependent on the spacecraft operation, such as attitude control and choice of telemetry formats and bit rate. In Figure 3 and 4, a number of orbit-dependent parameters are indicated so that one can more readily determine the times and latitudes at which moon-free airglow observations could be made from OGO-4. Airglow observations were made for five lunations beginning in late August 1967.

The spacecraft was in a near polar orbit (inclination = 86°) with perigee of about 400 km and apogee of 930 km. Consecutive orbits with a period of about 98 minutes crossed the equator at intervals of 24.5° longitude; orbits of consecutive days were offset from those of the previous day by about 8°. The plane of the orbit moved slowly with respect to the sun such that the local time changed 6 minutes each day, or 12 hours in 4 months. See Figure 5. The latitude of perigee moved slowly, making one complete revolution in about 103 days.

The field of view of the main body photometer had a nominal half angle of 5^{o} (for precise values, see Table 3) corresponding to a measurement diameter at the various levels of emission as given in Table 5.

The spacecraft was generally earth oriented so that the +Z axis (the main body photometer axis) pointed to the center of the earth, as defined by horizon scanners, and, in the presence of sunlight, the -Y axis always was in the sun-earth plane. The most notable exception was the period in August 1967, when the spacecraft was spun about its -Y axis which was pointed toward the sun. Occasionally, at other times, the earth-stabilized mode would be lost for an orbit or two, but was soon restored.

Since there was not sufficient telemetry capacity available to give experiments the sample rate they required at all times, the telemetry system was time-shared by the use of different telemetry formats, some of which gave high sample rates to certain experiments, but none to others. In general, for a 48 hour period, format 00 was used, followed by a 48 hour period in which a variety of formats were commanded. Each day a format entirely devoted to the various spacecraft monitors was scheduled for one orbit.

The Main Body Photometer had a barely adequate sample rate (two useful samples per second) when the spacecraft data handling system used format 00 at the 4 kbs (kilobits

TABLE 5

altitude of emission	spacecraft at 400 km	spacecraft at 900 km
0 km	70 km	160 km
100	52	145
300	17	110

Diameter of the area observed for various altitudes of emission and various altitudes of the spacecraft.

per second) rate. At other rates and formats there was an adequate number of samples so that noise could be more readily identified and deleted (see Table 6).

MAIN BODY PHOTOMETER DATA

The summary maps prepared for the 6300 A airglow represent about 3/4th of the data available at low latitudes and are described in Table 7. Of these, four have been selected for inclusion here. (Color Plates 1-4) These represent various local times in the September-December period. Color prints of all 19 maps may be obtained from the author (Reed and Blamont, 1972) or the National Space Science Data Center.

Most of the maps are centered on the two-day format 00 period from which there were generally at least 10 orbits of data per day. Each map includes some additional data from the days preceding and following, from which there are generally less than 5 orbits per day. In the occasional cases where two orbits of data were available for a single longitude, the orbit which seemed a better match to the neighboring orbits was used. The summary maps have space for a maximum of 44 orbits; the ones prepared each contain data from 14 to 41 orbits. In the north-south direction, photometer readings are made at approximately half-degree intervals. The longitudes of orbit from which data were used are indicated by the location of the orbit numbers at the top of each map.

TABLE 6

Bit rate	Main Commutator			Sub-Commutator
	Format 00	Format 12	Format 15	
4 kbs	3.47	41.7	27.8	0.027
16 kbs	13.9	167	111	0.108
64 kbs	55.6	667	444	0.434

Data rate in samples per second. The four analog outputs and one digital output from each photometer were on the Main Commutator. The remaining words were on the Sub-Commutator.

TABLE 7

MAP	START			END			NO of ORBITS	LOCAL TIME
	MONTH DAY	TIME	ORBIT	MONTH DAY	TIME	ORBIT		
1	8/30	0844	482	9/2	0537	524	31	0310
2	9/4	0254	552	9/7	0619	598	32	0246
3	9/7	1049	601	9/9	1345	632	16	0228
4	9/25	2219	873	9/28	1100	910	32	0044
5	9/28	1847	915	10/2	0617	966	32	0026
6	10/3	2102	990	10/6	1929	1033	35	2358
7	10/7	1441	1045	10/10	1622	1090	30	2337
8	10/10	1917	1092	10/13	1111	1131	27	2320
9	10/22	2120	1270	10/26	0708	1320	33	2210
10	10/26	1812	1327	10/30	0400	1377	34	2146
11	10/30	1957	1387	11/1	1438	1413	14	2127
12	11/2	1128	1426	11/5	0635	1467	26	2107
13	11/18	0027	1655	11/20	1757	1695	13	1932
14	11/22	2143	1727	11/25	0033	1758	30	1908
15	11/27	0240	1789	11/30	0104	1832	31	1838
16	12/25	2332	2215	12/28	1522	2254	29	0336
17	12/29	0403	2262	12/30	2243	2288	19	0318
18	1/1	2312	2318	1/5	2020	2375	26	0246
19	1/6	0052	2378	1/10	0746	2441	41	0219

Periods in 1967-8 covered by the set of 19 maps. Start and end times are given by month, day of month, hour and minute of Universal Time (GMT). Local time in hours and minutes is average local time at the geodetic equator. The number of orbits used in the preparation of each map is stated. Map 5, 10, 14, and 17 are reproduced with this paper.

In these maps the contours of the airglow are indicated as the boundaries of the various colors. The minimum-B equator at 300 km (Stassinopoulos 1970) is plotted as a heavy black line. The local time on the map is a nominal local time. All points on the map were observed within 20 minutes of the stated time, the differences being due to the inclination of the orbit, the range in latitude (corresponding to a 27 minute variation in local time), and to the movement of the plane of the orbit (0.417 minutes change of local time per orbit). A plot of local time and of Ap (average amplitude of magnetic activity) is found in Figure 5. Observations from August through November were taken as the satellite moved through the earth's shadow from north to south, so that local times at the top of the map are earlier than those at the bottom. In December and January, the satellite was moving from south to north as it passed through the earth's shadow, so that local times at the bottom of these maps are earlier.

Some of the maps do include data from which a substantial background of moonlight has been subtracted. The four maps included here are from moon-free periods.

In all maps there are areas for which no useful photometer data is available. The lack of data may be for any of several reasons:

(1) Interference due to energetic particles penetrating the spacecraft and striking the photomultiplier window. (See Reed et al 1967 and Fowler et al 1968). This is important in the region of the South Atlantic magnetic anomaly.

(2) The earth and lower atmosphere within the field of view of the photometer may be sunlit. For this reason no data south of 25^{o} latitude are included in map 14, nor are data south of 0^{o} latitude included in map 13.

(3) No data were received. This may be due to planned operations of the spacecraft to permit sharing of the limited telemetry among the various users, to occasional loss of attitude control, or to problems in data collection and processing.

(4) The data was not processed for the maps by the experimenter. This is true for all realtime data and for a small amount of playback data in which there were special problems.

In the discussion of these maps, frequent references are made to ground-based observations. The locations of ground and rocket-borne observations and the approximate parths of ship and aircraft observations are given in Figure 6, accompanied by Table 8. In Table 8 the geomagnetic latitude is computed for a north pole with geographic coordinates of 11.435^{o} geocentric co-latitude and -69.761^{o} east longitude (Mead 1970). The McIlwain parameter, L, was obtained for an altitude of 250 km for 1968.0 using the Pogo (8/69) coefficients given in Cain and Sweeney (1970). The WDC-A column indicates that the station

TABLE 8

	LOCATION	GEOGRAPHIC Lat	Long	GEOMAG Lat	L 250 km	WDC -A	IQSY
1	Fritz Peak	39 54	-105 29	48.7	2.4	X	X
2	Sendai (Tokhatta)	38 6	140 33	28.1	1.3	x	x
3	Ashkhabad (Vannovskaya)	37 57	58 6	30.5	1.4	x	x
4	Fan Mtn	37 53	- 78 42	49.1	2.6		
5	Wallops Island	37 50	- 75 29	49.1	2.6		
6	Sounion	37 42	24 0	36.1	1.4		
7	Granada	37 0	- 3 30	40.8	1.5		
8	Cactus Peak	36 5	-117 49	43.2	1.9		
9	Dodaira	36 0	139 12	25.9	1.3	x	x
10	Gifu	35 27	137 2	25.2	1.3	x	x
11	Maruyama	35 1	139 58	25.0	1.3	x	x
12	Aso	32 53	131 1	22.2	1.2	x	x
13	Sacramento Peak	32 43	-105 45	41.6	1.8	x	
14	White Sands	32 24	-106 23	41.2	1.8		
15	Tucson	32 15	-110 50	40.5	1.7		
16	Kitt Peak	31 57	-111 36	40.1	1.7	x	x
17	Kagoshima	31 30	130 30	20.7	1.2		
18	Sde Boker	30 54	34 48	27.4	1.2		
19	Canary Islands	28 0	- 16 0	34.3	1.3	x	
20	Mt Abu	24 36	72 43	15.4	1.1	x	x
21	Tamanrassett	22 48	5 32	25.2	1.1	x	
22	Barking Sands	22 1	-159 8	21.7	1.2		
23	Haleakala	20 42	-156 15	21.0	1.2	x	x
24	Poona	18 31	73 52	9.2	1.0	x	x
25	Arecibo	18 24	- 66 54	29.8	1.5		
26	Agadez	16 58	7 59	19.0	1.0		
27	Debre Zeit	8 45	38 36	5.0	1.0	x	
28	Lwiro	- 2 16	28 49	-3.5	1.1	x	
29	Jicamarca	-11 57	-76 52	-0.7	1.1		
30	Huancayo	-12 3	-75 20	-0.7	1.1	x	
31	Chacaltaya	-16 18	-68 12	-4.9	1.1		
32	Makatea	-16 25	-148 20	-13.9	1.1	x	x
33	Aitutaki	-18 54	-159 48	-18.5	1.1		
34	Tsumeb	-19 13	17 42	-18.3	1.4	x	x
35	Townsville	-19 15	146 45	-28.2	1.3	x	
36	Tongatapu	-21 12	175 12	-25.6	1.3		
37	Monumento Rodoviario	-22 30	-44 0	-12.2	1.2		
38	Roma	-29 42	27 42	-30.5	1.7		
39	Woomera	-30 58	136 54	-40.9	1.8		
40	San Juan (El Leoncito)	-31 32	-68 33	-20.2	1.2		
41	Camden	-34 0	150 24	-42.3	2.0	x	
42	Adelaide	-34 52	138 57	-44.6	2.1		

was listed in the Catalog of Data on Solar-Terrestrial Physics, (WDC-A, 1971) as having 6300A airglow data. The IQSY column indicates that the station participated in IQSY observations (Shapley and Roach 1970).

Figure 6, drawn to the same scale as are the color plates, shows the location of the stations in Table 8. Dashed lines indicate the approximate paths of various shipboard and aircraft expeditions. Thin lines represent apex latitudes (VanZandt et al 1972), and the heavy solid line is the minimum-B equator for 300 km altitude.

A list of over 100 references for these observations may be found in Reed, 1972.

TROPICAL ARCS

Location

The most striking feature of the maps from the OGO-4 data are the broad belts of high emission rate in the vicinity of the equator. In Color Plate 1, the northern arc is well developed at most longitudes. There is a persistent tendency for the northern arc to be weak near -30° longitude. The ionosphere over the southern part of C.P. 1 is sunlit, as indicated by the curves in Figure 7, showing the height of the earth's shadow above the surface of the earth.

In Color Plate 2, both the northern and southern arcs are present with a typical location corresponding to about 30° dip angle. By midnight, as seen in Color Plate 3, the

arcs have moved toward each other and have partially merged. The intensities diminish in an irregular manner in the early morning hours, degenerating into irregular patches which show little repeatability from day to day as shown in Color Plate 4.

From ground observations the northern tropical arc was first identified as such by Barbier and Glaume (1960). They noted from data at Tamanrasset (Algeria) that the 6300A airglow was often in the form of an east-west arc, usually moving from the north to the south during the course of the night, sometimes continuously, sometimes disappearing and reforming anew slightly to the south of its old position. Using observations from Tamanrasset, Agadez, a simultaneous airplane flight, and earlier observations from Lwiro (Delsemme and Delsemme 1960), and noting the patterns of airglow that could be computed from various ionosonde stations, Barbier et al (1961) postulated a pair of tropical arcs of world wide extent. Since then, they have been observed more or less extensively from Haleakala (Hawaii) and from Mt. Abu and Poona (India). They have also been observed by other airplane flights, from shipboard, and from satellites. Selected references may be found in Table 9, in the recent reviews by Silverman (1970) and Brasher & Hanson (1970), and an extensive list in Reed (1972).

North-South Dissymmetry

The north-south dissymmetry in the tropical arc is especially marked in the maps from October 22 to November 5,

of which Color Plate 2 is an example. The southern arc grew progressively weaker over this time span. This might be considered a seasonal effect if one looks at ground observations which are summarized in Table 9. The behavior described by the references of this table in some cases was very marked, as at Tamanrasset, and in others was only a moderate tendency, as in the shipboard observations.

Even when arcs are present on both sides of the equator, their location and shape may or may not be symmetrical and similar. See especially C.P. 2 and 3. Weill et al (1968) reported that in December 1966 - January 1967 at Debre Zeit, Ethiopia, near the dip equator at about 40^{o} longitude "the northern and southern arcs do not only differ in their intensities and seasonal variations. They also differ notably in width, and in their nocturnal movement and intensity variations. They move into the equatorial region at different times, and on individual nights their behavior seems unrelated."

Equatorial Minimum

Early in the evening, the 6300A emissions between the tropical arcs is at very low values. This had been noted indirectly by observations near the magnetic equator at Huancayo (Peru) when Silverman and Casaverde (1961) reported that the midnight maximum value was about a factor of 4 or 5 greater than the minimum observed for the night, considerably greater than for other non-auroral stations.

TABLE 9

PLACE	PERIOD OF OBSERVATION	BEHAVIOR	REFERENCE
Tamanrasset-Agadez	1957-1962	Max in winter	Weill, 1967; Barbier 1961
Lwiro, Africa	1958-1959	Max in Feb-Apr	A. & D. Delsemme 1960
Haleakala, Hawaii	1961-1965	Max in Sept-Nov & Mar-Apr	Steiger 1967
Poona, India	Jan-Mar 1964	Max in Jan	Chiplonkar & Tillu 1970
Mt. Abu, India	1964-1967	Max in Dec-Jan	Pal 1971
SHIPBOARD AND AIRCRAFT			
Japan-Antarctica	Nov-Dec 1959 Feb-Apr 1960	Strong N arc Strong S arc	Nakamura 1961
Africa	Nov 1960 Mar 1961	Strong N arc Strong S arc	Barbier et al 1961
W of South America	May-Nov 1962 Feb-May 1965	Strong N arc Strong S arc	Davis and Smith 1965 Greenspan 1966
Alaska-Samoa	Oct 1968	Strong N arc	Glass et al 1970

At nearby Jicamarca, Peterson and VanZandt (1969) noted that during 1967 and 1968, early evening values typically were low, and occasionally were essentially zero. This they attributed to the great height of the F2 layer. Measurements by the Jicamarca Radar Observatory indicated that "after sunset the F2-layer rises rapidly from its daytime level and occasionally the height of the layer maximum, h_{max}, reaches an altitude exceeding 600 km. After staying at this altitude for a period ranging from a few minutes to several hours, the F2-layer drops in height, typically at a rate of about 20 $msec^{-1}$. Occasionally h_{max} drops as low as 250 km. The total height excursions of the F2-layer during any one night is typically about 150 km, although excursions as large as 300 km have been observed".

The tendency for the emission rates in the equatorial minimum at longitudes between 0^{o} and 120^{o} to be somewhat greater than those at other longitudes is apparent on C.P. 2 and also on the other maps of these lunations. This is undoubtedly influenced by the shape of the earth's magnetic field; maps of L at 300 km (Stassinopoulos 1970) show that L is less than 1 at the min-B equator at 300 km at longitudes between about 50^{o} and 150^{o}.

Magnetic Activity

The most notable magnetic storm in the periods covered by these maps occurred on September 28-30. Data for only a

few orbits are available for September 28 and 29; SAR-arcs were observed on orbits 915 and 923. The most noticeable feature distinguishing this map (C.P. 3) from the others of that lunation is that the southern arc at longitudes between 60^{o} and 160^{o} is weak or absent, while on the others (especially maps 6, 7, and 8) the southern arc tends to be stronger than the northern arc.

Other observers have noted that at Tamanrasset intensities were generally depressed for several hours after a sudden commencement, and the arc structure disrupted (Barbier 1962, Weill and Christophe-Glaume, 1967). At Debre Zeit, Weill, et al., (1968) reported that the 6300A emission rose to record intensities at the peak of a storm before midnight, and then fell within 2 hours to record lows. King (1968) has noted that during disturbed conditions, the ionospheric equatorial anomaly is less developed in that the equatorial arch is narrower and the crest-trough ratio of critical frequency smaller than normal.

Solar Cycle

In terms of the solar cycle, the data observed from OGO-4 are representative of smoothed sunspot numbers of about 100. The long term observations at Tamanrasset (Weill 1967) and at Haleakala (Steiger 1967, Smith and Steiger 1968) indicate that for low sunspot numbers, less than 30 as in 1963-1965, the average intensities decreased

markedly, by at least 2/3, the mean dip latitude of the arcs decreased by at least 6^{o}, and that the arc structure tended to degenerate into patches.

MID-LATITUDE AIRGLOW

Post-Twilight Decay

An examination of the values of the 6300A emission at latitudes between those of the tropical arcs and the aurora shows that the values are high in the twilight (C.P. 1) and decrease after sunset until sometime after midnight (C.P. 2 and C.P. 3). The northern part of C.P. 4 continues to show low post-midnight values, except near 0^{o} to -120^{o} longitude, which will be discussed later. The ionosphere in the southern part of C.P. 4 is sunlit to the extent indicated by the shadow heights given in Figure 7.

Observations at latitudes and times which are free from aurora and tropical arcs show that the 6300A emission usually decays monotonically from its twilight value over a period of several hours, often extending beyond midnight. Chamberlain (1958, 1961) reviewed a number of earlier observations, computed the rates that might be contributed by the resonance scattering of sunlight and by decay of the nighttime F-region through dissociative recombination of O_2^+, and concluded that the latter process was the principal one involved. Pal (1970) noted that decay rates at Mt. Abu varied with season; the profiles he computed through use of Chamberlain's formula agreed fairly well with observations. Swider (1967) reviewed

basic ionospheric processes and concluded that a simple decay of the lower F-region gave reasonable results for red-line emissions such as were observed at Haute Provence and Camden. Noxon and Johanson (1970) have made detailed studies using simultaneously measured 6300A rates and electron density profiles from Boston (U.S.A.). Brown and Steiger (1972) studied decay rates using Haleakala data, and found that the post-twilight decay rate apparently has no seasonal, solar-cycle, or magnetic activity dependence. The initial post-twilight value of emission, observed at Haute Provence (Barbier 1959) and at Haleakala (Steiger 1967) does have a solar cycle variation, being low at sunspot minmum. Annual averages at Haute Provence do show a positive correlation with sunspot number (Barbier 1965).

Predawn Behavior

On all three maps of the late August lunation, there are regions at mid-latitudes in which the emission rate is greater than 100 R and the general level seems to be somewhat greater than are midnight levels. However, the location of the regions of enhancements changes from map to map. For the late December lunation all maps are noticeably brighter to the south at all except about 0 to 60° longitude.

Conjugate Phenomena

On Color Plates 2 and 4, and on the other maps of those lunations, there is a region of enhanced emission extending down from the north and centered near -60° longitude. In some instances

its boundary is noticeably parallel to the min-B equator, although in Color Plate 2 this is somewhat obscured by the day to day variations. Generally there is not a noticable increase in 3914A emissions above the approximately 20R background due to the band emissions and reflected zodiacal and starlight normally appearing through this filter at mid-latitudes.

Predawn enhancements were frequently observed at Haute Provence France (Barbier 1959). These and other observations were discussed by Chamberlain (1961). Cole (1965) noted that the time and location of these enhancements corresponded to sunrise in the conjugate F-region and postulated that the enhanced airglow was due to photoelectrons which had traveled along the magnetic lines of flux to the nighttime ionosphere. Since then, maps have been calculated to indicate when and where such enhancements might be expected to occur (Deehr 1969); the direct contribution to 6300A emissions from photoelectrons has been found to be from 10 to 100 R depending on local conditions (Noxon 1971), and various observations have indicated that the predawn enhancement is in part related to an increase in radiative recombination of O_2^+, associated with a change in height of the ionosphere (Noxon and Johanson 1970, Nichol 1970, Schaeffer 1971). A third source of predawn enhancement is the creation of excited O by thermal electrons, whose temperature has been increased by the transfer of energy from the conjugate point.

SUMMARY

The low latitude observations of the 6300A emissions of OI reveal geographic and diurnal variations for a northern fall-winter season during a time ofhigh solar acitivity (smoothed sunspot numbers of about 100). In some areas, these observations can be extended to other times and seasons by use of the ground based observations. The major features observed are:

1. Tropical red arcs. These are apparent immediately after sunset, although development ofthe arcs at Atlantic longitudes is slow. Early evening values at the magnetic equator are low (often less than 25 R) with a longitude correlation with L (McIlwain parameter). The southern (summer) arc is weak except over Africa and the Atlantic. Even here it is noticeably weakening during the two week period of late October - early November. During the night the two arcs move toward the equator and partially merge. In the early morning hours, intensities in the tropics decrease, and the arc structure degenerates into patches.

2. Mid-latitude. The mid-latitude values to the north and south of the tropical arcs reach a maximum shortly after sunset and generally diminish until after midnight. Morning values are generally higher than midnight values, particularly in the south in the December-January series.

3. Conjugate phenomena. An increase in intensities corresponding to sunlit conjugate areas is apparent in the evening (C.P. 2) as well as in the morning (C.P. 4).

ACKNOWLEDGEMENTS

The authors thank Mr. Jacques Pacquet of the Centre National de la Recherche Scientifique (France) for the programming and data reduction resulting in the microfilm plots upon which the maps in this paper are based.

REFERENCES

Arvesen, J.C., R.N. Griffin, Jr., and B.D. Pearson, Jr., "Determination of Extraterrestrial Solar Spectral Irradiance from a Research Aircraft", Applied Optics, 8, 2215, 1969.

Barbier, D., "Recherches sur la Raie 6300 de la Luminescence Atmospherique Nocturne", Ann. Géophys., 15, 179, 1959.

Barbier, D., "Les Variations d'Intensité de la Raie 6300 Å de la Luminescence Nocturne", Ann. Géophys., 17, 3, 1961.

Barbier, D., "Airglow and Earth Storm", J. Phys. Soc. Jap., 17, Supp. A-1, 255, 1962.

Barbier, D., "Variations de l'Intensité des Principales Radiations de la Luminescence Atmospherique Nocturne Avec le Cycle Solaire", Ann. Géophys., 21, 265, 1965.

Barbier, D., and J. Glaume, "Les Radiations de l'Oxygène 6300 et 5577 Å de la Luminescence du Ciel Nocturne dans une Station de Basse Latitude", Ann. Géophys., 16, 319, 1960.

Barbier, D., G. Weill, and J. Glaume, "L'Émission de la Raie Rouge du Ciel Nocturne en Afrique", Ann. Géophys. 17, 305, 1961.

Bauernschub, J.P., "Mechanisms for Spacecraft Optical Instrumentation", NASA Technical Note TN-D-3008, 1965.

Brasher, W.E., and W.B. Hanson, "Distributions of Nighttime F-Region Molecular Ion Concentrations and 6300-Å Nightglow Morphology", Radio Sci., 5, 1325, 1970.

Broadfoot, A.L., and K.R. Kendall, "The Airglow Spectrum, 3100-10,000 A", J. Geophys. Res., 73, 426, 1968.

Brown, W.E., and W.R. Steiger, "6300 Å Quantum Efficiency of the Recombination Mechanism in the Night-time F Layer", Planet. Space Sci., 20, 11, 1972.

Cain, J.C., and R.E. Sweeney, "Magnetic Field Mapping of the Inner Magnetosphere", J. Geophys. Res., 75, 4360, 1970.

Chamberlain, J.W., "Oxygen Red Lines in the Airglow. I. Twilight and Night Excitation Processes", Astrophys. J., 127, 54, 1958.

Chamberlain, J.W., "Physics of the Aurora and Airglow", Academic, New York, 1961.

Chiplonkar, M.W. and A.D. Tillu, "The F-Layer Component of the 5577 Å Emission of the Night Airglow at Poona", Ann. Géophys., 26, 213, 1970.

Code, A.D., "Stellar Energy Distribution", Stellar Atmospheres, edited by J. L. Greenstein, U. of Chicago Press, Chicago 1960.

Cole, K.D., "The Predawn Enhancement of 6300 Å Airglow", Ann. Géophys., 21, 156, 1965.

Davis, T.N., and L.L. Smith, "Latitudinal and Seasonal Variations in the Night Airglow", J. Geophys. Res., 70, 1127, 1965.

Deehr, C.S., "The Predawn Enhancement of 6300 Å (OI) Airglow: Morphology and Variation with Solar Activity", Ann. Géophys., 25, 867, 1969.

Delsemme, A. and D. Delsemme, "La Raie Rouge du Ciel Nocturne a l'Équateur", Ann. Géophys., 16, 507, 1960.

Fowler, W.B., E.I. Reed, and J.E. Blamont, "Effects of Energetic Particles on Photomultipliers in Earth Orbits up to 1500 km", GSFC X-613-68-486, Goddard Space Flight Center, Greenbelt, Md., Dec. 1968. (N69-18074)

Fowler, W.B., E.I. Reed, and J.E. Blamont, "Bidirectional Reflectance of the Moonlit Earth", Applied Optics, 10, 2657, 1971.

Glass, N.W., J.H. Wolcott, R.L. Wakefield, and R.W. Peterson, "Airborne Observations of the Night Airglow", Ann. Géophys., 26, 179, 1970.

Greenspan, J.A., "Synoptic Description of the 6300 Å Nightglow near 78° West Longitude", J. Atmos. Terr. Phys., 28, 739, 1966.

Harris, D.L., "Photometry and Colorimetry of Planets and Satellites", Planets and Satellites, edited by G.P. Kuiper and B.M. Middlehurst, U. of Chicago Press, Chicago, 1961.

King, J.W., "Airglow Observations and the Decay of the Ionospheric Equatorial Anomaly", J. Atmos. Terr. Phys., 30, 391, 1968.

Mead, G.D., "International Geomagnetic Reference Field 1965.0 in Dipole Coordinates", J. Geophys. Res., 75, 4372, 1970.

Nakamura, T., "Latitude Effect of the Oxygen Red Line of Night Airglow and Its Relation with the Ionospheric F-Layer", Rept. Ionos. Sp. Res. Japan, 15, 245, 1961.

Nichol, D.G., "The Pre-Dawn Enhancement of λ6300Å Airglow at Higher Midlatitudes", Planet. Space Sci., 18, 1335, 1970.

Noxon, J.F., "Interpretation of F Region Nightglow", The Radiating Atmosphere, edited by B.M. McCormac, Reidel, Dordrecht, Holland, 1971.

Noxon, J.F., and A.E. Johanson, "Effect of Magnetically Conjugate Photoelectrons on OI(6300 Å), Planet. Space Sci., 18, 1367, 1970.

Pal, S.R., "Post-Twilight Decay of 6300 Å Emission", Ann. Géophys., 26, 791, 1970.

Pal, S.R., "Covariation in 6300 Å and 5577 Å Emissions in Nightglow", Planet. Space Sci., 19, 1087, 1971.

Peterson, V.L., and T.W. VanZandt, "O(^{1}D) Quenching in the Ionospheric F-Region", Planet, Space Sci., 17, 1725, 1969.

Ramsey, R.C., "Spectral Irradiance from Stars and Planets, above the Atmosphere, from 0.1 to 100.0 Microns", Applied Optics, 1, 465, 1962.

Reed, E.I., "Bibliography of Observations of 6300A Night Airglow at Latitudes from 40°N to 40°S, GSFC X-625-72-172 Goddard Space Flight Center, Greenbelt, Md. 1972.

Reed, E.I., and J.E. Blamont, "Some Results Concerning the Principal Airglow Lines as Measured from the OGO-II Satellite", Space Res., 7, 337, 1967.

Reed, E.I., and J.E. Blamont, "OGO-4 Observations of the 6300 A Night Airglow from 40°N to 40°S: A Set of 19 Color Maps", GSFC X-625-72-173, Goddard Space Flight Center, Greenbelt, Md., 1972.

Reed, E.I., W.B. Fowler, C.W. Aitken, and J.F. Brun, "Some Effects of Mev Electrons on the OGO II (POGO) Airglow Photometers, GSFC X-613-67-132, Goddard Space Flight Center, Greenbelt, Md., 1967.

Reed, E.I., W.B. Fowler, and J.E. Blamont, "Functional Characteristics of the OGO Main Body Airglow Photometer, GSFC X-625-72-174, Goddard Space Flight Center, Greenbelt, Md., 1972.

Roach, F.E., "Manual for Photometric Observations of the Airglow During the International Geophysical Year, NBS Report 5006, National Bureau of Standards, Washington, D.C., 1956. Also in Ann. IGY, 4, Part 2, Pergamon, 1957.

Schaeffer, R.C., "The Role of Recombination in the Pre-Dawn Enhancement of λ6300 Å [OI] Airglow", J. Atmos. Terr. Phys., 33, 437, 1971.

Shapley, A.H. and F.E. Roach, "IQSY Data Review: Night Airglow", Ann. IQSY, 6, MIT Press, Cambridge, Mass., 1970.

Silverman, S.M., "Night Airglow Phenomenology", Space Sci. Rev., 11, 341, 1970.

Silverman, S.M., and M. Casaverde, "Behavior of the 6300 O I Line at Huancayo", J. Geophys. Res., 66, 323, 1961.

Smith, L.L., "Comparison of [OI] 6300 A and [OI] 5577 A Observations from Haleakala, Hawaii, and the OGO-4 Satellite in 1967", Final Report, Contract No. Y-40670, Battelle Memorial Institute, Pacific Northwest Laboratories, Richland, Washington, 1970.

Smith, L.L. and W.R. Steiger, "Night Airglow Intensity Variations in the [OI] 5577 A, [OI] 6300 A, and NaI 5890-96 A Emission Lines", J. Geophys. Res., 73, 2531, 1968.

Stassinopoulos, E.G., "World Maps of Constant B, L. and Flux Contours", NASA SP-3054, 1970.

Steiger, W.R., "Low Latitude Observations of Airglow", Aurora and Airglow, edited by B. M. McCormac, Reinhold, New York, 1967.

Swider, W., "On the Decay of the Ionospheric Airglow 6300 Å Line at Night", Space Res., 7, 516, 1967.

Warnecke, G., E.I. Reed, W.B. Fowler, E.R. Kreins, L.J. Allison, and J.E. Blamont, "Meteorological Results from Multi-Spectral Photometry in Airglow Bands by the OGO-4 Satellite", J. Atmos. Sci., 26, 1329, 1969.

Weill, G.M., "Airglow Observations near the Equator", Aurora and Airglow, edited by B.M. McCormac, Reinhold, New York, 1967.

Weill, G., and J. Christophe-Glaume, "Ciel Nocturne et Aurores de Basse Latitude en Période d'Orage Magnétique", Ann. Géophys., 23, 317, 1967.

Weill, G., M. Fehrenbach, N. Morguleff, and J. Christophe-Glaume, "The Forbidden Lines of OI and NI in the Night Airglow at the Magnetic Equator", Ann. Géophys., 24, 109, 1968.

World Data Center A, NOAA, Boulder, Colorado, Catalogue of Data on Solar-Terrestrial Physics, Upper Atmosphere Geophysics Report UAG-15, July 1971.

VanZandt, T. E., W.L. Clark, and J.M. Warnock, "Magnetic Apex Coordinates: A Magnetic Coordinate System for the Ionospheric F_2 Layer", J. Geophys. Res., 77, 2406, 1972.

FIGURE CAPTIONS

Figure 1. Responsivity of the main body photometer relative to the laboratory calibration of May 1966.

Figure 2. Comparison of simultaneous observations of airglow from OGO-4 and the Haleakala Observatory, Maui, Hawaii. The non-zero intercept is attributed to imperfect corrections for the background emissions of the E-region and the sky.

Figure 3. Observing periods and locations for the descending (north-to-south) half of the OGO-4 orbit. In the times and latitudes indicated by the shaded areas, the sub-satellite point was moonlit. The time and latitude of full moon is indicated by the small circles. The latitude of perigee and apogee as a function of time is indicated. At times and latitudes within the large misshapen oval, the satellite was in the earth's shadow.

Figure 4. Observing periods and locations for the ascending half (south-to-north) half of the OGO-4 orbit. See caption for Figure 3.

Figure 5. Map coverage, local hour at the equator, and average amplitude of magnetic activity (A_p).

Figure 6. Locations of other observations of 6300A airglow. Lines for the minimum-B equator at 300 km and for Apex latitudes are also included.

Figure 7. Height of the umbra above the sub-satellite point as a function of latitude for the first and last orbits C.P. 1 and 4.

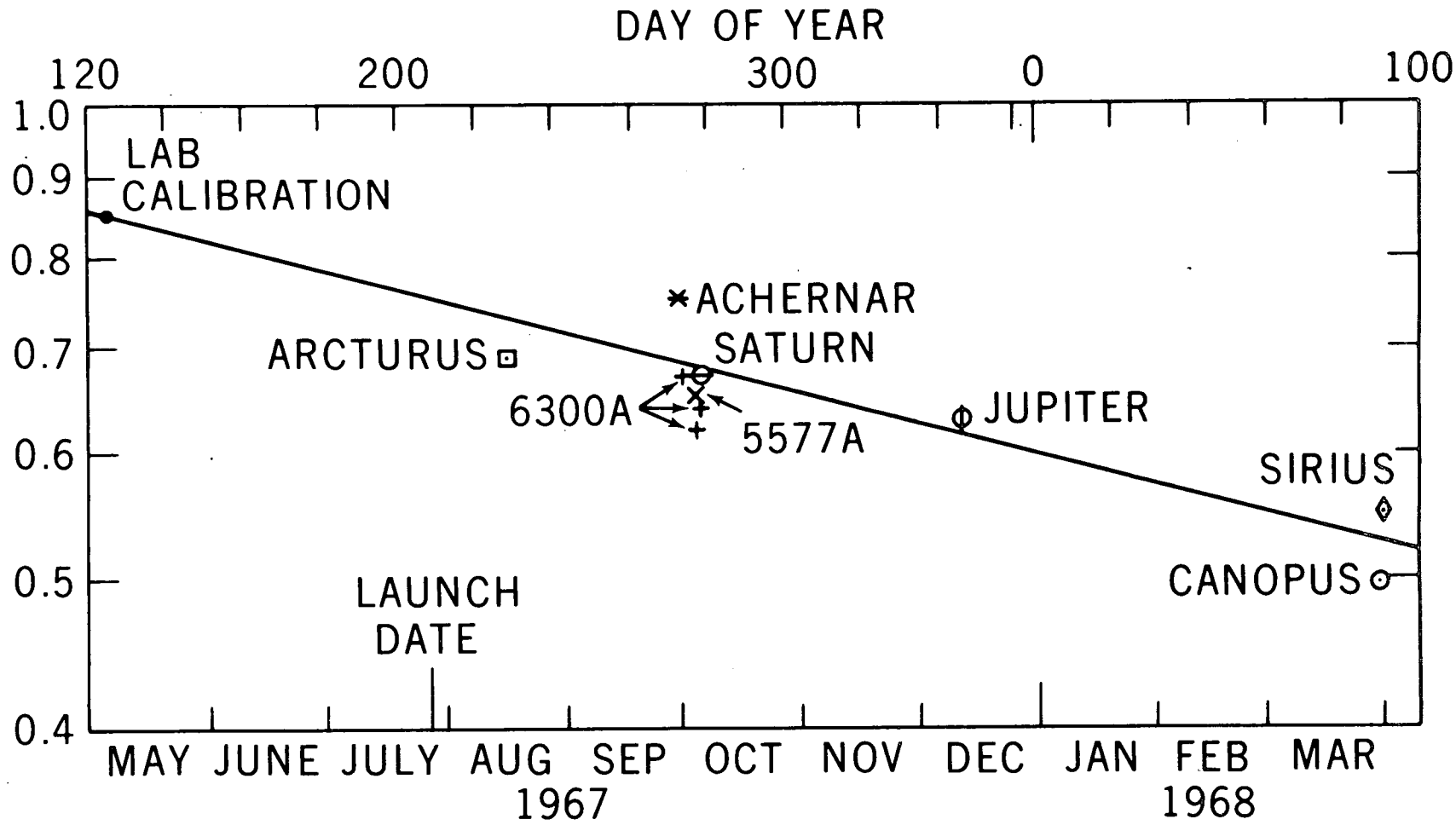
DAY OF YEAR
120
200
300
0
100
1.0
0.9
0.8
0.7
0.6
0.5
0.4
LAB
CALIBRATION
ACHERNAR
SATURN
ARCTURUS
6300A
5577A
JUPITER
SIRIUS
CANOPUS
LAUNCH
DATE
MAY JUNE JULY AUG SEP OCT NOV DEC JAN FEB MAR
1967
1968

Fig. 1

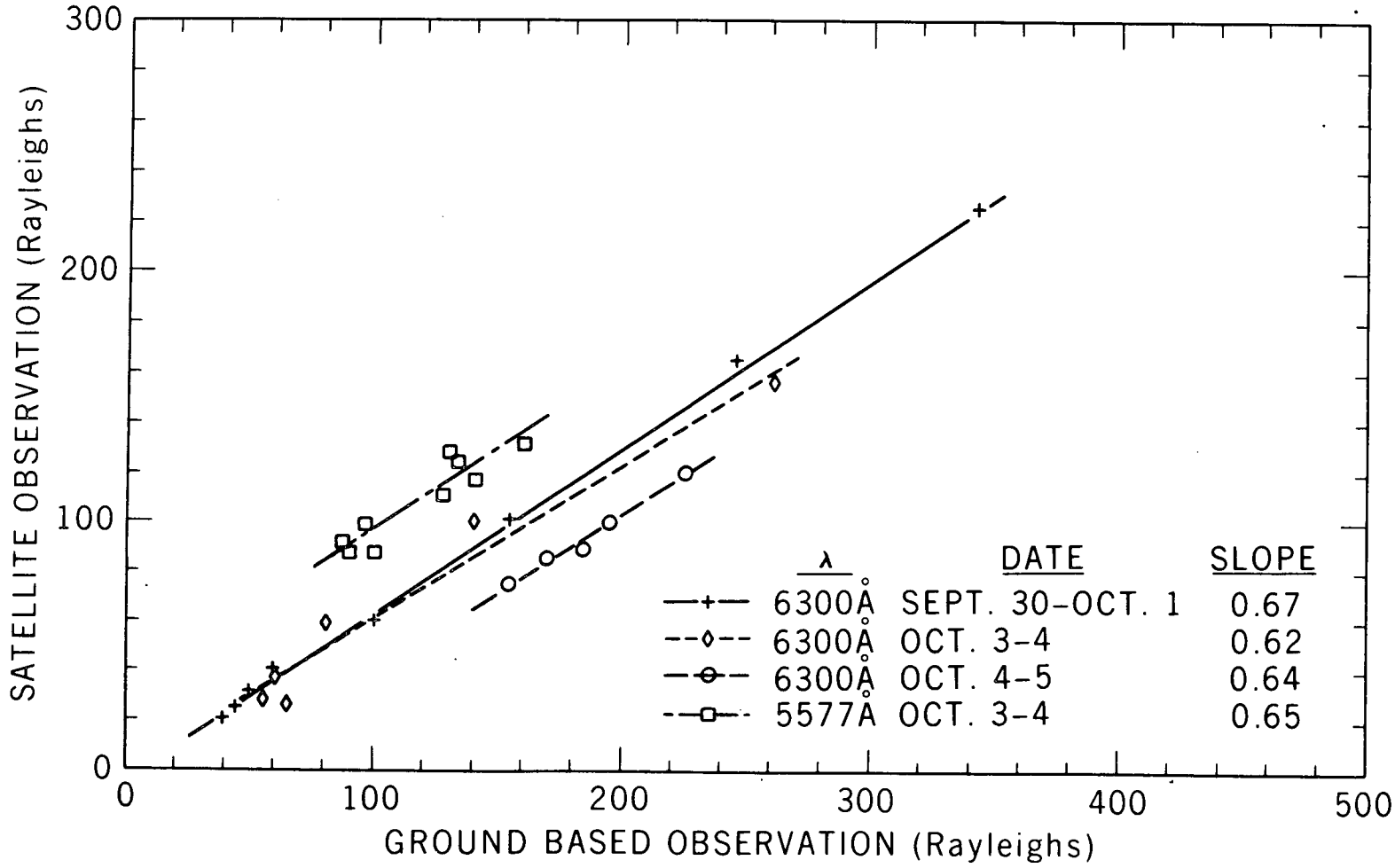
SATELLITE OBSERVATION (Rayleighs)
GROUND BASED OBSERVATION (Rayleighs)
0
100
200
300
400
500
λ DATE SLOPE
6300Å SEPT. 30-OCT. 1 0.67
6300Å OCT. 3-4 0.62
6300Å OCT. 4-5 0.64
5577Å OCT. 3-4 0.65

Fig. 2

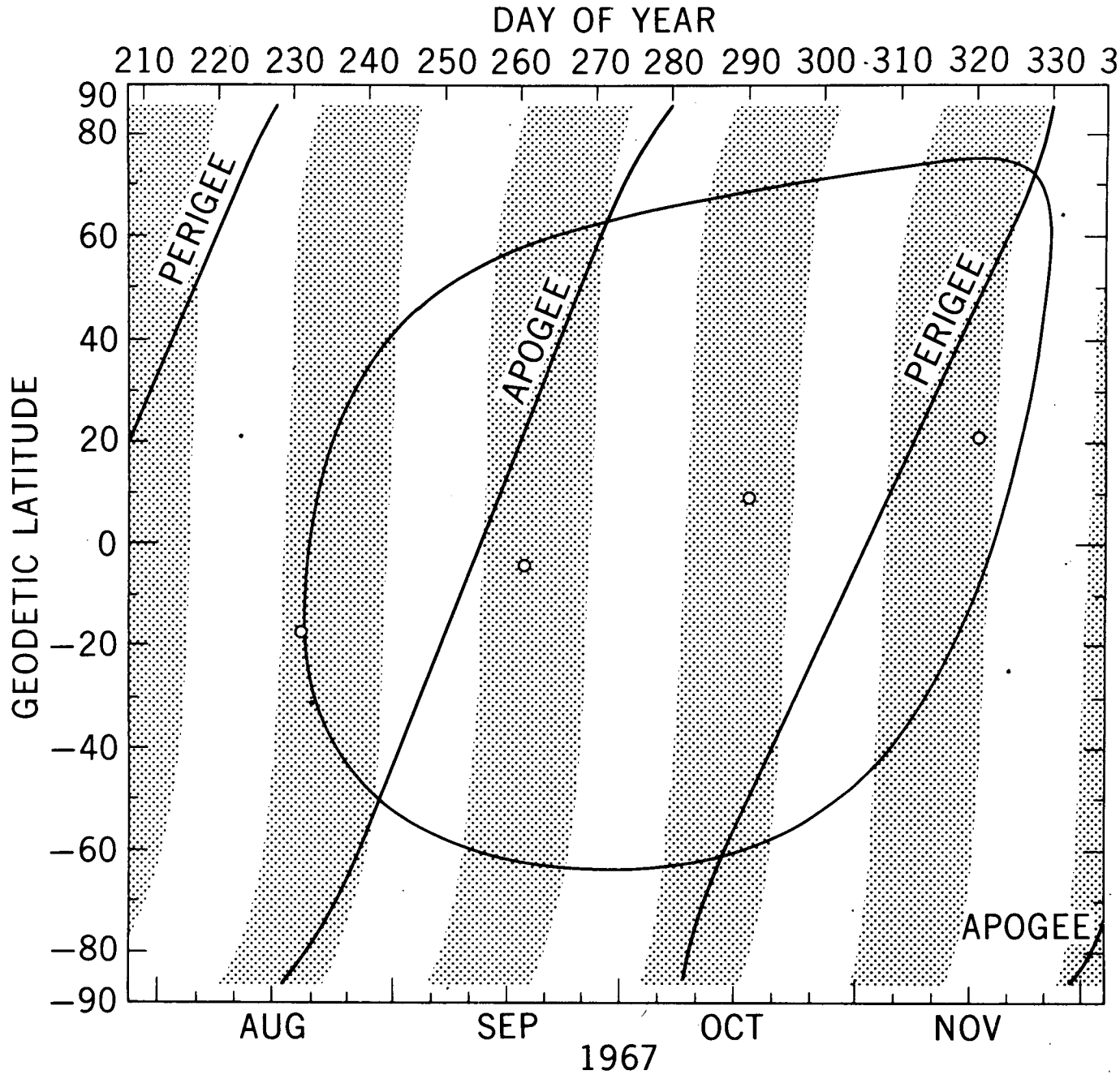
DAY OF YEAR
210 220 230 240 250 260 270 280 290 300 310 320 330 337
90
80
60
40
20
0
−20
−40
−60
−80
−90
GEODETIC LATITUDE
PERIGEE
APOGEE
PERIGEE
APOGEE
AUG
SEP
OCT
NOV
1967

Fig. 3

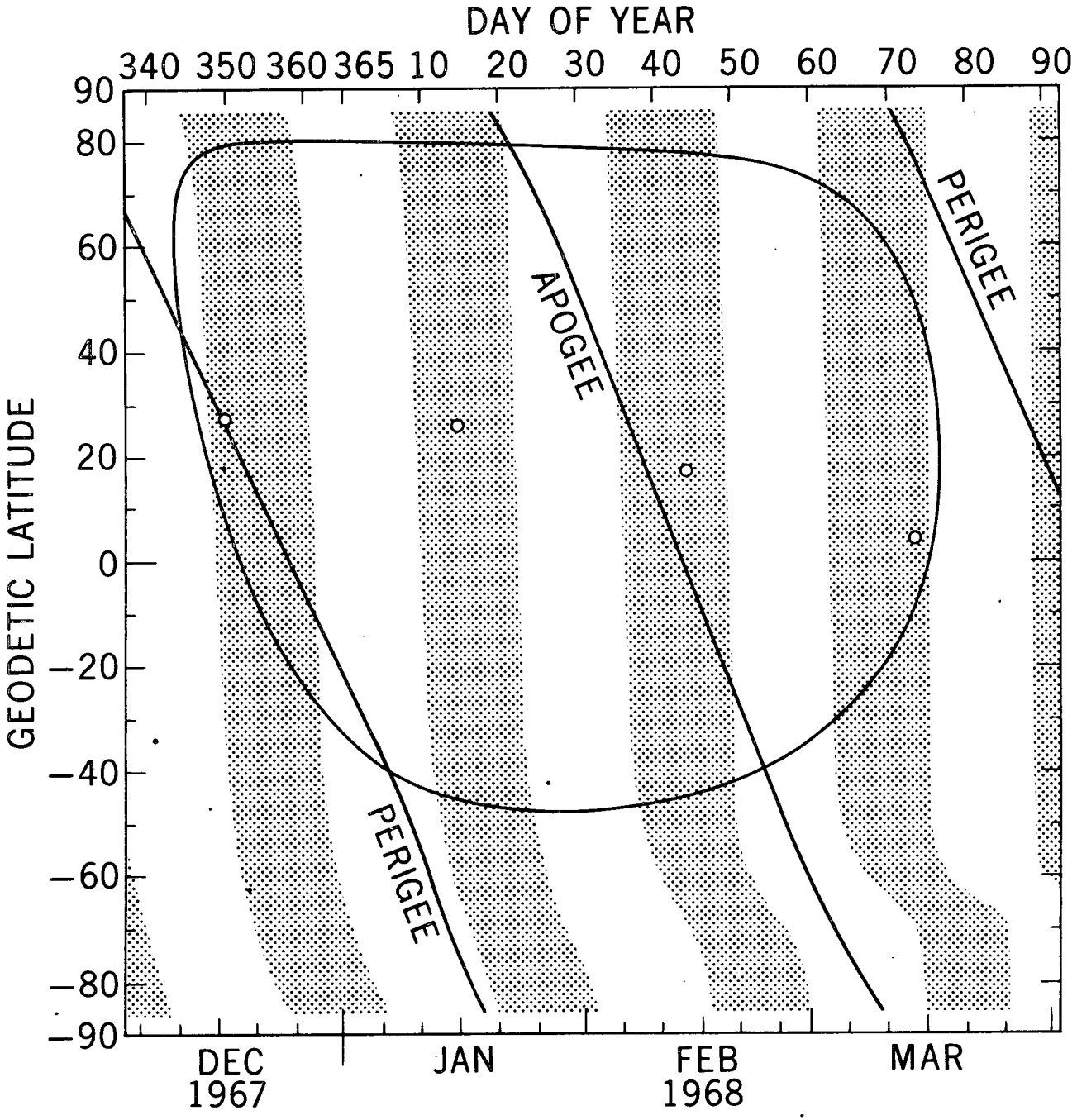
DAY OF YEAR
340 350 360 365 10 20 30 40 50 60 70 80 90
90
80
60
40
20
0
−20
−40
−60
−80
−90
GEODETIC LATITUDE
APOGEE
PERIGEE
PERIGEE
DEC
1967
JAN
FEB
1968
MAR

Fig. 4

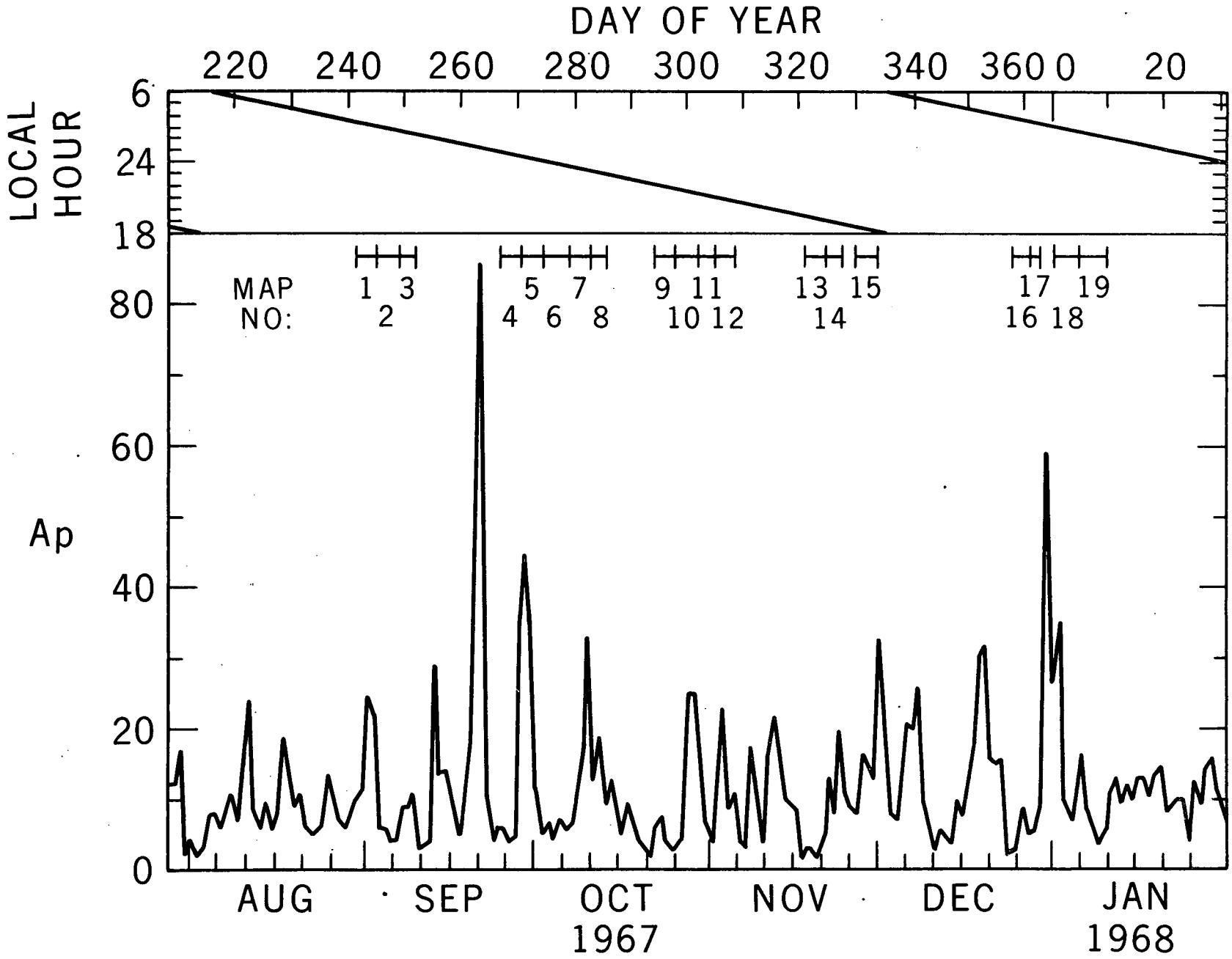
DAY OF YEAR
220
240
260
280
300
320
340
360
0
20
LOCAL HOUR
6
24
18
MAP NO:
1 3
2
5 7
4 6 8
9 11
10 12
13 15
14
17 19
16 18
Ap
80
60
40
20
0
AUG
SEP
OCT
1967
NOV
DEC
JAN
1968

Fig. 5

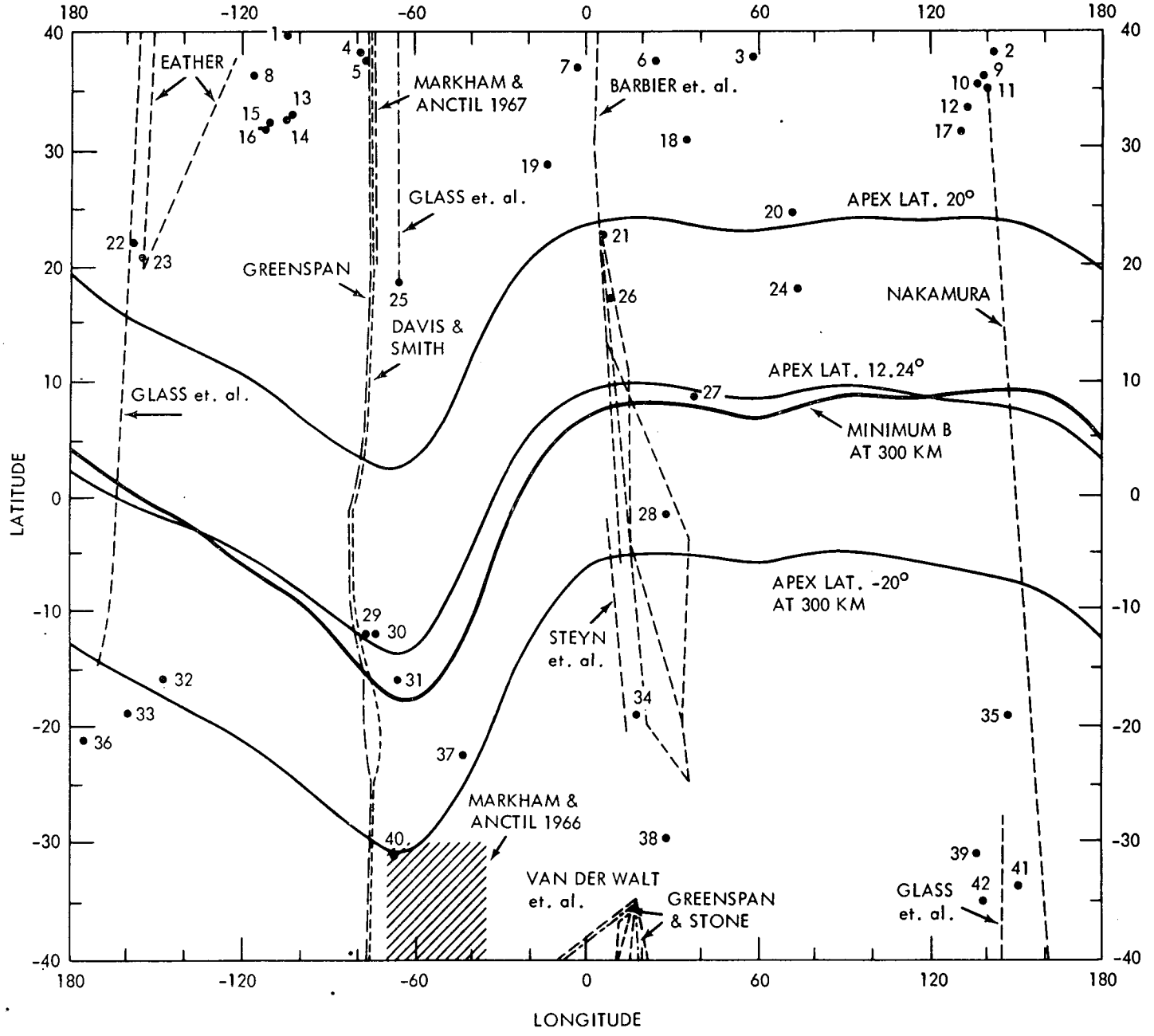
180
-120
-60
0
60
120
180
40
30
20
10
0
-10
-20
-30
-40
LATITUDE
LONGITUDE
EATHER
MARKHAM &
ANCTIL 1967
BARBIER et. al.
GLASS et. al.
APEX LAT. 20°
GREENSPAN
DAVIS &
SMITH
NAKAMURA
GLASS et. al.
APEX LAT. 12.24°
MINIMUM B
AT 300 KM
APEX LAT. -20°
AT 300 KM
STEYN
et. al.
MARKHAM &
ANCTIL 1966
VAN DER WALT
et. al.
GREENSPAN
& STONE
GLASS
et. al.
1
2
3
4
5
6
7
8
9
10
11
12
13
14
15
16
17
18
19
20
21
22
23
24
25
26
27
28
29
30
31
32
33
34
35
36
37
38
39
40
41
42

Fig. 6

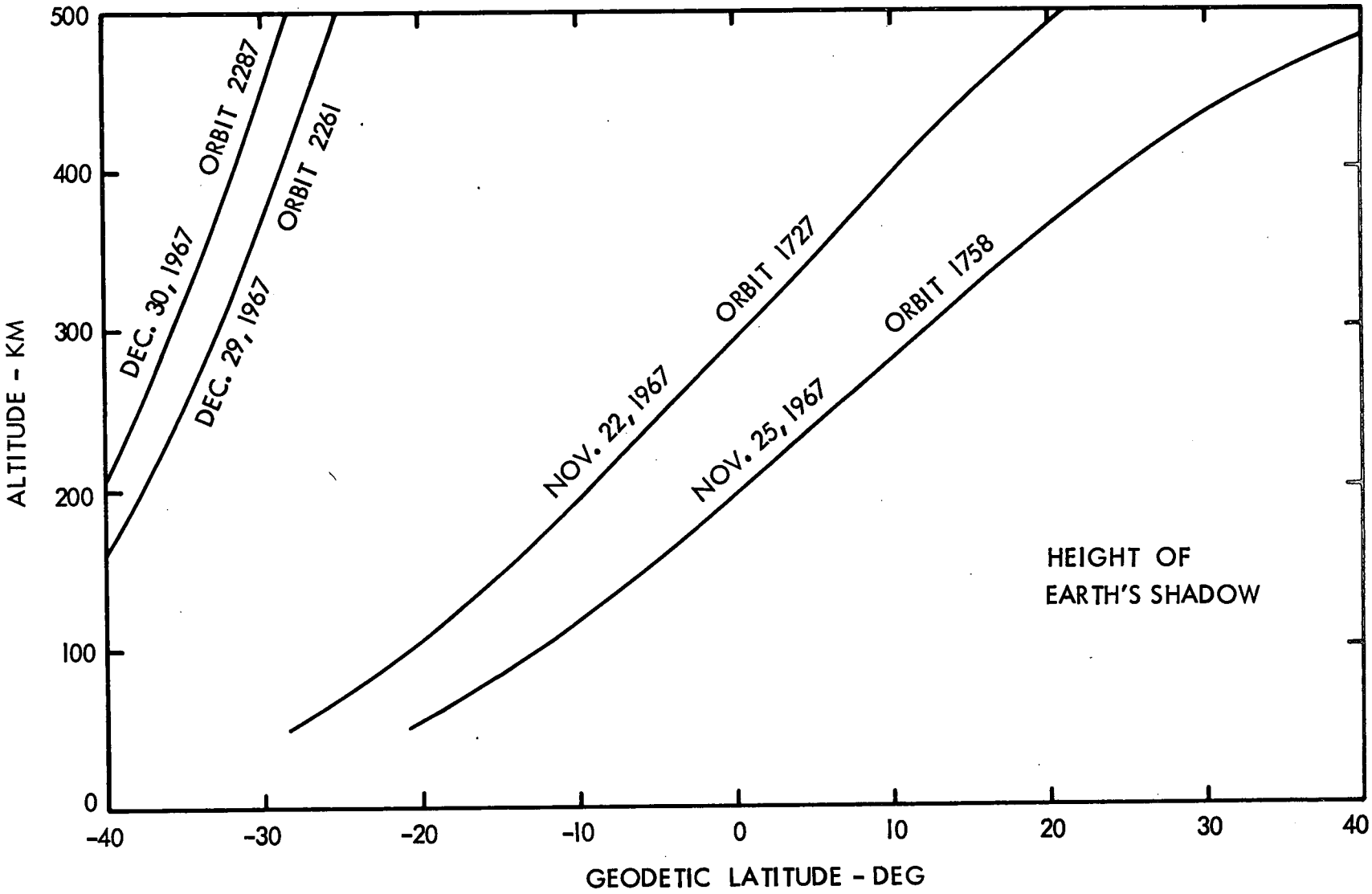
500
400
300
200
100
0
ALTITUDE - KM
-40
-30
-20
-10
0
10
20
30
40
GEODETIC LATITUDE - DEG
DEC. 30, 1967
ORBIT 2287
DEC. 29, 1967
ORBIT 2261
NOV. 22, 1967
ORBIT 1727
NOV. 25, 1967
ORBIT 1758
HEIGHT OF
EARTH'S SHADOW

Fig. 7

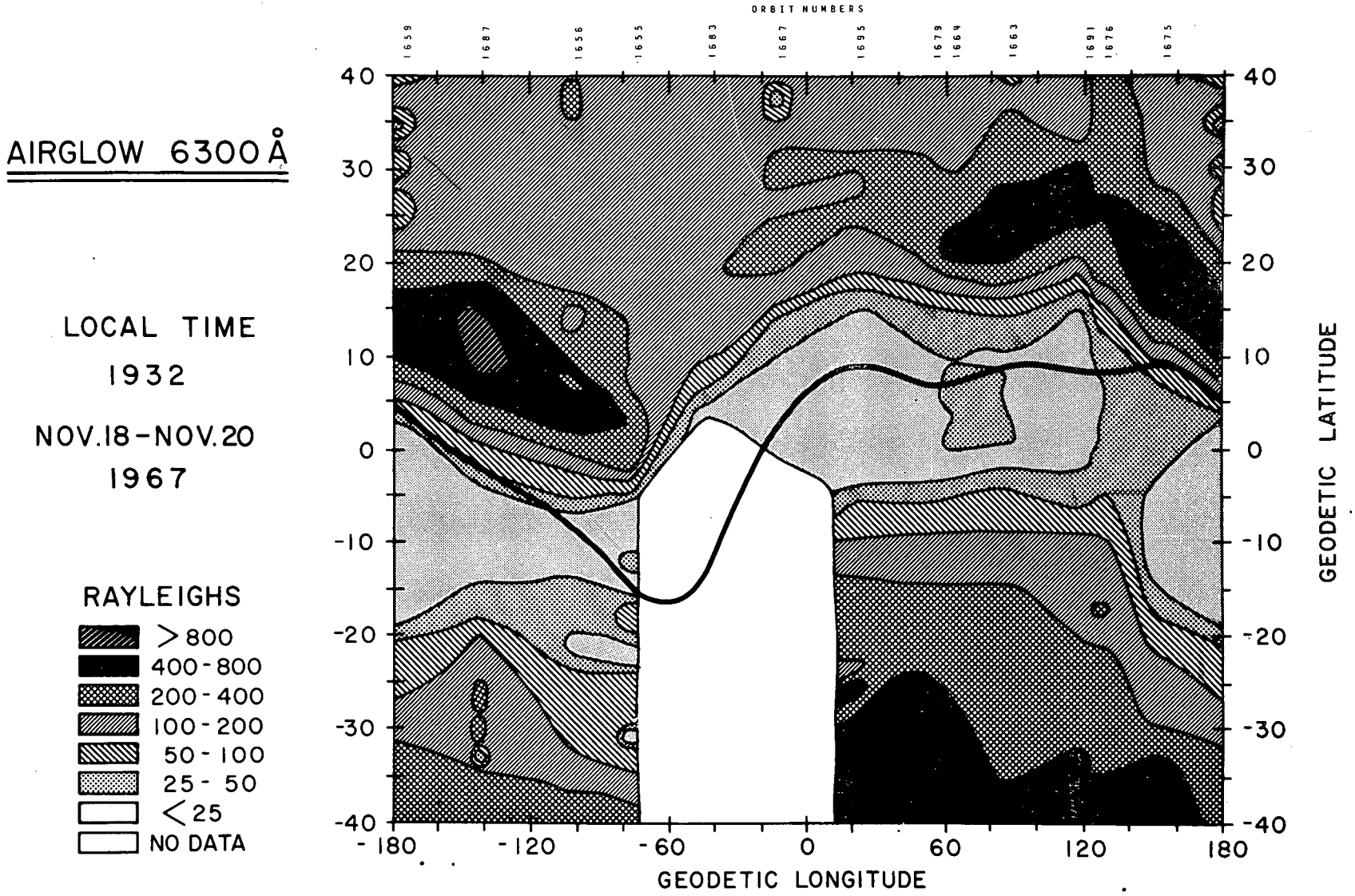
AIRGLOW 6300 Å
LOCAL TIME
1932
NOV.18-NOV.20
1967
RAYLEIGHS
>800
400-800
200-400
100-200
50-100
25-50
<25
NO DATA
ORBIT NUMBERS
1659
1687
1656
1655
1683
1667
1695
1679
1664
1663
1691
1676
1675
40
30
20
10
0
-10
-20
-30
-40
-180
-120
-60
0
60
120
180
GEODETIC LONGITUDE
GEODETIC LATITUDE

Plate 1

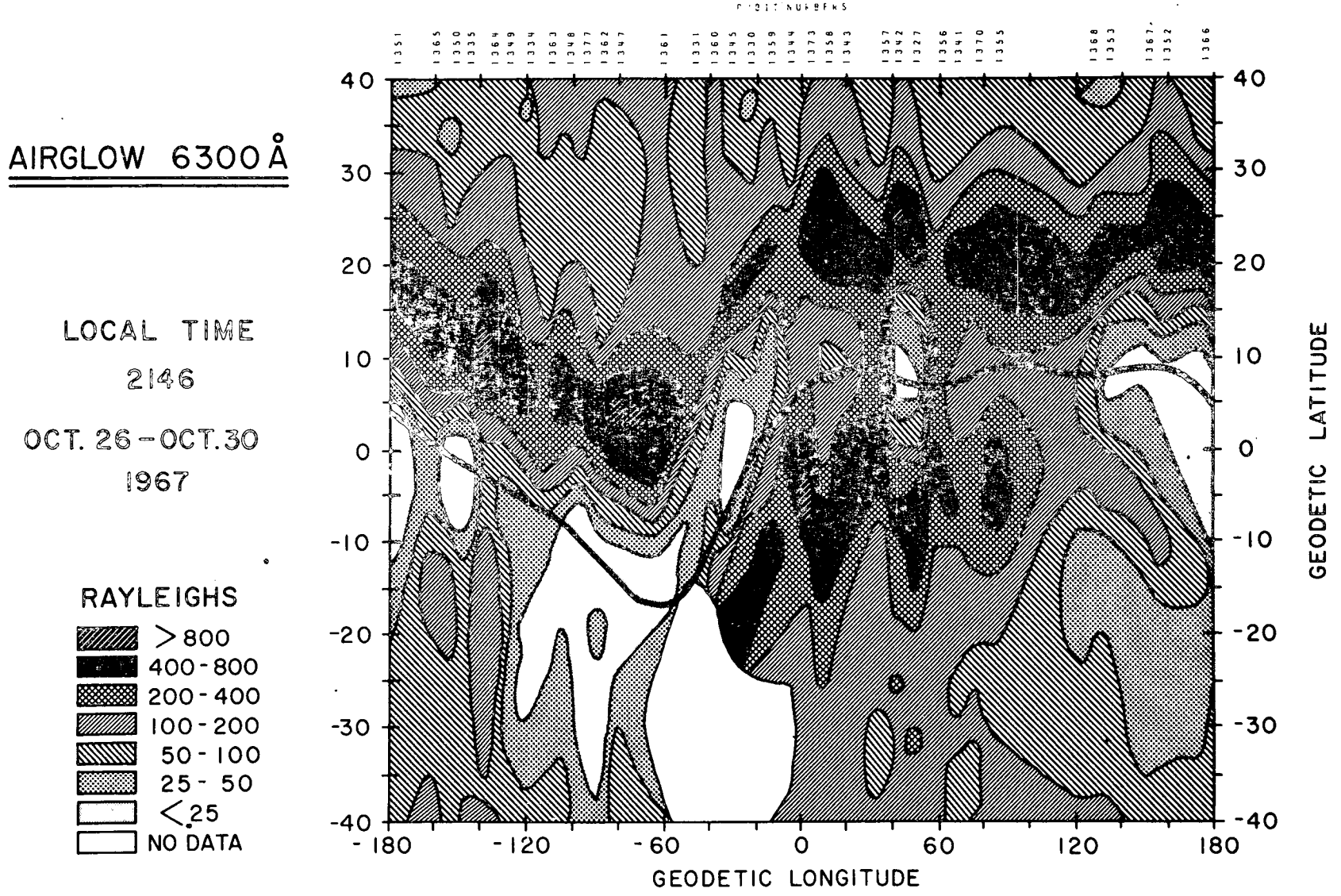
AIRGLOW 6300 Å
LOCAL TIME
2146
OCT. 26 – OCT. 30
1967
RAYLEIGHS
> 800
400 - 800
200 - 400
100 - 200
50 - 100
25 - 50
< 25
NO DATA
PLOT NUMBERS
1351 1365 1350 1335 1364 1349 1334 1363 1348 1377 1362 1347 1361 1331 1360 1345 1330 1359 1344 1373 1358 1343 1357 1342 1327 1356 1341 1370 1355 1368 1353 1367 1352 1366
40
30
20
10
0
-10
-20
-30
-40
-180
-120
-60
0
60
120
180
GEODETIC LONGITUDE
GEODETIC LATITUDE

Plate 2

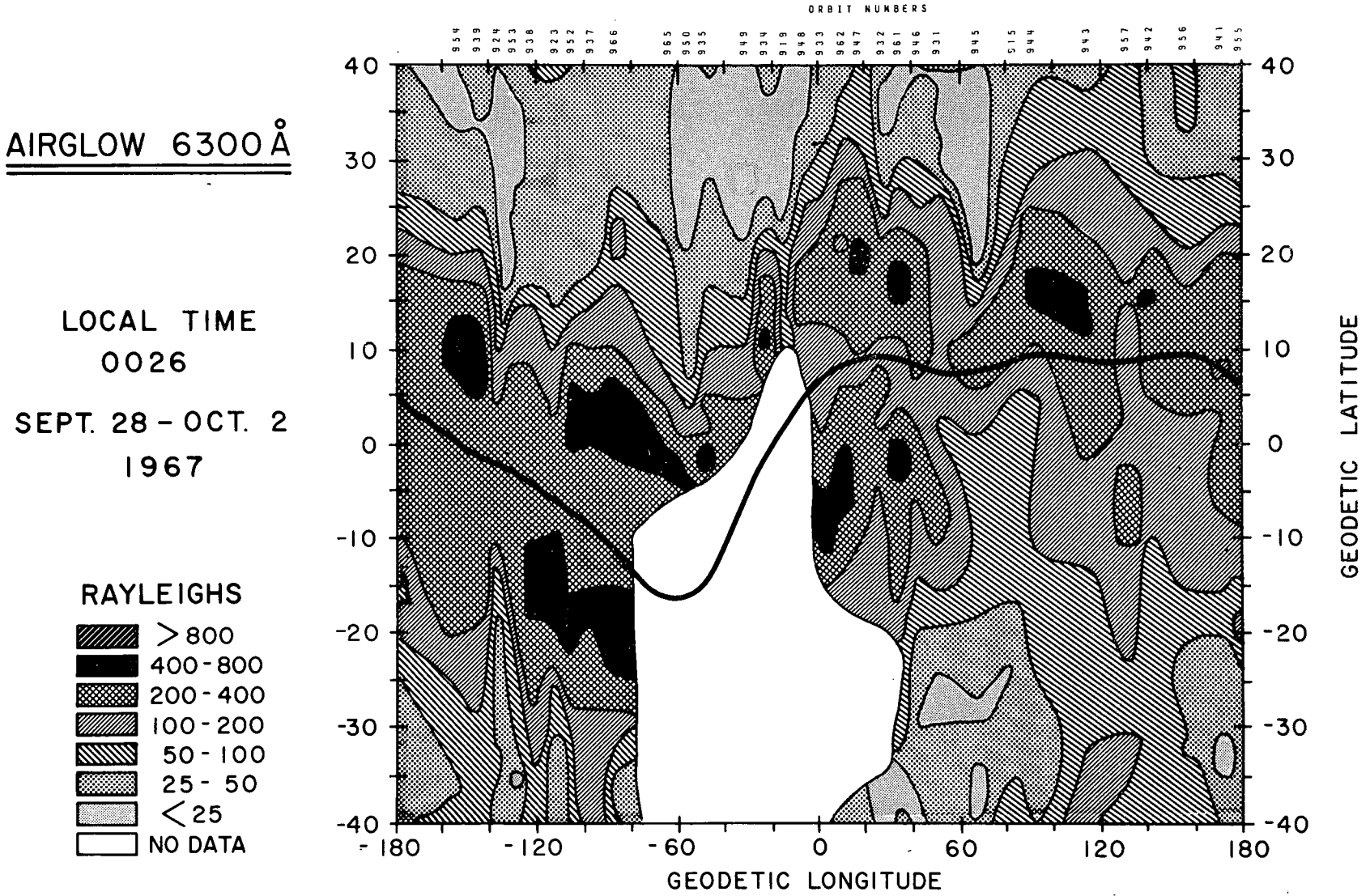
AIRGLOW 6300 Å
LOCAL TIME
0026
SEPT. 28 - OCT. 2
1967
RAYLEIGHS
> 800
400 - 800
200 - 400
100 - 200
50 - 100
25 - 50
< 25
NO DATA
ORBIT NUMBERS
954 939 924 953 938 923 952 937 966 965 950 935 949 934 919 948 933 962 947 932 961 946 931 945 515 944 943 957 942 956 941 955
40
30
20
10
0
-10
-20
-30
-40
-180
-120
-60
0
60
120
180
GEODETIC LONGITUDE
GEODETIC LATITUDE

Plate 3

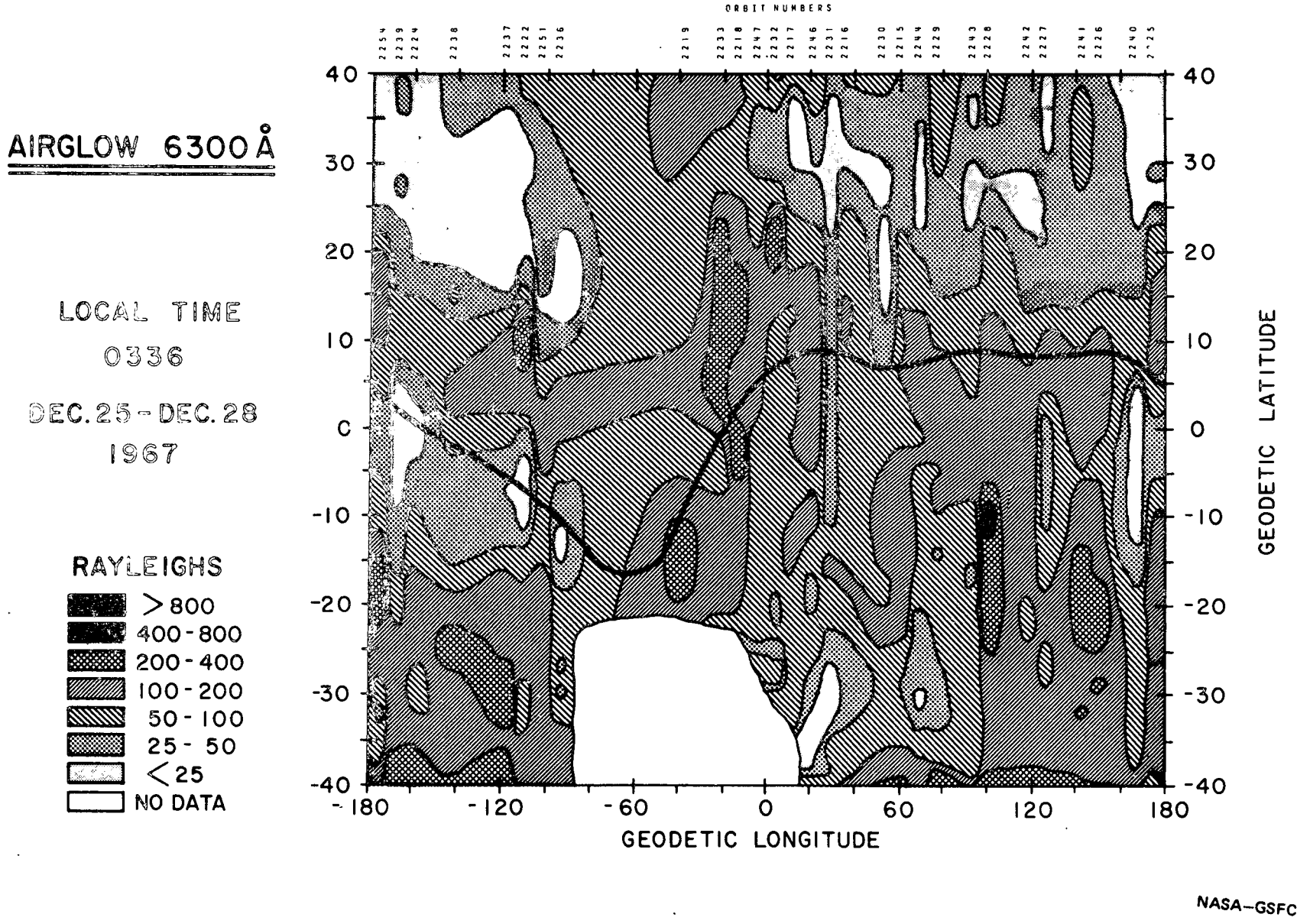
AIRGLOW 6300 Å
LOCAL TIME
0336
DEC. 25 - DEC. 28
1967
RAYLEIGHS
> 800
400 - 800
200 - 400
100 - 200
50 - 100
25 - 50
< 25
NO DATA
ORBIT NUMBERS
2254 2239 2224 2238 2237 2222 2251 2236 2219 2233 2218 2247 2232 2217 2246 2231 2216 2230 2215 2244 2229 2243 2228 2242 2227 2241 2226 2240 2225
40
30
20
10
0
-10
-20
-30
-40
-180
-120
-60
0
60
120
180
GEODETIC LONGITUDE
GEODETIC LATITUDE
NASA-GSFC

Plate 4